Analog Gopinath Motion Observer for Velocity Self-Sensing

Austin Gaspar, Eduardo Rocha, Kshitij Girigoudar

Introduction and Prelab (KG)

A. Objectives (KG)

The main goal of this project was to implement a Gopinath observer and evaluate the performance of the observer by analytical and experimental methods.

The limitations in designing and implementing the observer were studied by using the estimation accuracy metric and dynamic stiffness. The effect of parameter estimation errors on estimation accuracy of observer was determined along with investigation of the state feedback motion controller performance with the observer estimated velocity feedback.

B. Equipment (KG)

The following equipment is used for this lab:

1. B&K dynamic signal analyzer
2. DC servo drive system
3. INSTEK function generator
4. PC with Pulse software
5. HP Oscilloscope
6. Digital multi Multi-meter (DMM)
7. Analog circuit breadboard and cables for connection

C. Prelab (KG)

The observer is represented in Fig. I.1. It can be clearly seen that the Gopinath observer is much more sensitive to parameter estimation error compared to Luenberger observer. Instead of using the measured outer state (velocity) as reference for convergence, the measured inner state (current) is used for the controller to track and estimate the outer state. There are two feedforward inputs to the observer. While one of the feedforward inputs can be either measured current or commanded current, the other feedforward would be the input voltage to the DC servo motor, which is the best feedforward signal available since it is the manipulated input of the system.

The state block diagram in Fig. I.1 shows a good design space representation of the physical intent of the controller, but is not particularly useful in implementing the controller. Each electronically simulated gain in Fig. I.1 will need to be equated to some op amp gain that is controlled by a user-defined resistance. This alternative implementation space state block

diagram is shown in Fig. I.2. The gains must be calculated such that positive feedback or saturation is avoided. Positive feedback has the potential of causing unstable behavior while op amp saturation gives rise to undesirable signals and commands which might damage equipment.

The observer gains for damping, stiffness, and integrated stiffness are tuned to achieve bandwidths of, 50 Hz, 10 Hz, and 2 Hz. To calculate estimates for the gains, the characteristic equation is utilized.

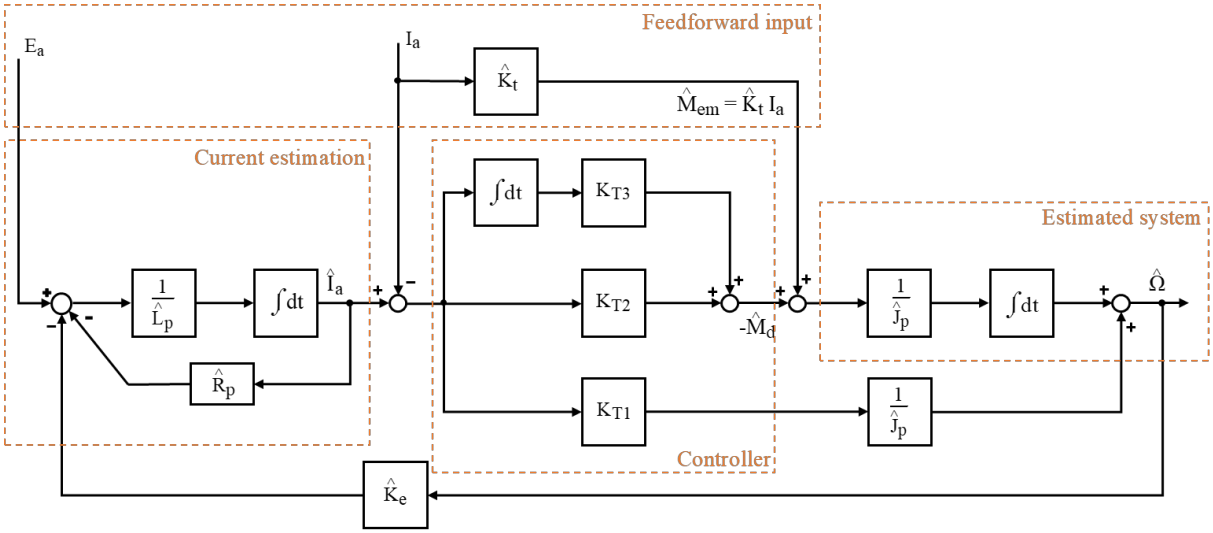

Fig. I.1. Simplified design state block diagram of Gopinath observer

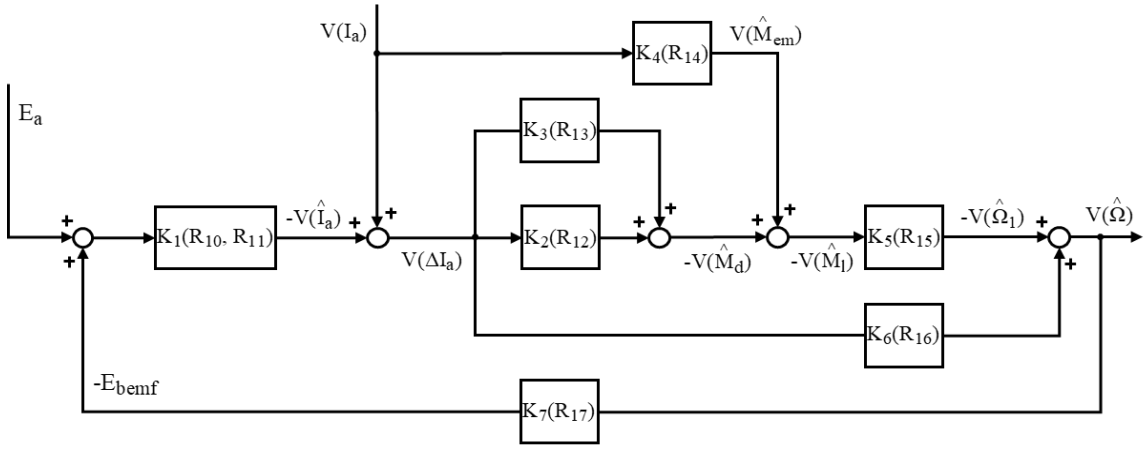

Fig. I.2. State block diagram of a Gopinath observer as implemented in lab

The estimation accuracy transfer function using the measured current i_a for the Gopinath observer is given by

$$\frac{\hat{\Omega}(s)}{\Omega(s)} = \frac{(K_{T1}\,s^2+K_{T2}\,s+K_{T3})\left(\frac{J_p\,s^2(L_p-\hat{L}_p)+J_p\,s(R_p-\hat{R}_p)}{K_T}+K_e\right)+\frac{\hat{K}_T}{K_T}J_p\,s^2(\hat{R}_p+s\,\hat{L}_p)}{\hat{J}_p\,\hat{L}_p\,s^3+(\hat{J}_p\,\hat{R}_p+\hat{K}_e\,K_{T1})\,s^2+\hat{K}_e\,K_{T2}\,s+\hat{K}_e\,K_{T3}}$$

(I.1)

It can be noted from equation I.1 that the Gopinath observer is slightly more difficult to analyze compared to the Luenberger observer. Even at low frequencies the estimation accuracy is not 1, but depends on the $K_e/\hat{K}_e$ ratio. The characteristic equation can be set equal to the desired bandwidth as shown in the following equation.

$$\hat{J}_p\,\hat{L}_p\,s^3+(\hat{J}_p\hat{R}_p+\hat{K}_e\,K_{T1})\,s^2+\hat{K}_e\,K_{T2}\,s+\hat{K}_e\,K_{T3}=(s+\omega_1)(s+\omega_2)(s+\omega_3) \quad \text{(I.2)}$$

In equation I.2, ω_1, ω_2, and ω_3 are the desired bandwidths expressed in radians per second. Equation I.2 can be transformed to yield the following equations:

$$K_{T1}=\frac{\hat{J}_p\times(2\pi\times50\times\hat{L}_p-\hat{R}_p)}{\hat{K}_e}=\frac{2.08\times10^{-5}\times(2\pi\times50\times2.88\times10^{-3}-2.96)}{0.067}=-6.38\times10^{-4}\left[\frac{\text{Nm-s}}{\text{A-rad}}\right] \quad \text{(I.3)}$$

$$K_{T2}=\frac{2\pi\times10\times(\hat{J}_p\times\hat{R}_p+\hat{K}_eK_{T1})}{\hat{K}_e}=\frac{2\pi\times10\times(2.08\times10^{-5}\times2.96+0.067\times-6.38\times10^{-4})}{0.067}=0.018\left[\frac{\text{Nm}}{\text{A}}\right] \quad \text{(I.4)}$$

$$K_{T3}=2\pi\times2\times K_{T2}=2\pi\times2\times0.018=0.222\left[\frac{\text{Nm-rad}}{\text{A-s}}\right] \quad \text{(I.5)}$$

These gains are implemented through a cascaded op-amp system, as shown in the circuit schematic shown in Fig. I.3. It is interesting to note that K_{T1} is negative for the chosen eigenvalues. The circuit was simulated and tested using TI spice to check for op amp saturation and general debugging of circuit.

The resistances in R_{10}, R_{11}, R_{12}, R_{13}, R_{14}, R_{15}, R_{16}, and R_{17} are calculated to achieve the gains using the equations below:

$$R_{11}=\frac{\hat{L}_p}{C_1\times\hat{R}_p}=\frac{2.88\times10^{-3}}{0.1\mu\text{F}\times2.96}=9.73\ [\text{k}\Omega] \quad \text{(I.6)}$$

$$R_{10}=\frac{\hat{R}_p}{k_a\times k_i}\times R_{11}=\frac{2.96}{5.05\times0.41}\times9.73\text{k}\Omega=13.91\ [\text{k}\Omega] \quad \text{(I.7)}$$

$$R_{12}=K_{T2}\times10\text{k}\Omega=0.018\times10\text{k}\Omega=176.5\ [\Omega] \quad \text{(I.8)}$$

$$R_{13}=\frac{1}{K_{T3}\times C_2}=\frac{1}{0.222\times4\mu\text{F}}=1.12\ [\text{M}\Omega] \quad \text{(I.9)}$$

$$R_{14} = \frac{1}{\hat{K}_t} \times 10k\Omega = \frac{1}{0.067} \times 10k\Omega = 149.25\ [k\Omega]$$

(I.10)

$$R_{15} = \frac{k_i \times \hat{J}_p}{k_v \times C_3} = \frac{0.41 \times 2.08\times10^{-5}}{0.016 \times 0.1\mu F} = 5.33\ [k\Omega]$$

(I.11)

$$R_{16} = \frac{k_i \times \hat{J}_p}{k_v \times K_{T1}} \times 10k\Omega = \frac{0.41 \times 2.08\times10^{-5}}{0.222 \times -6.38\times10^{-4}} \times 10k\Omega = 8.35\ [k\Omega]$$

(I.12)

$$R_{17} = \frac{\hat{K}_e}{k_a \times k_v} \times 10k\Omega = \frac{0.067}{5.05 \times 0.016} \times 10k\Omega = 8.29\ [k\Omega]$$

(I.13)

Analog Gopinath Motion Observer for Velocity Self-Sensing

Austin Gaspar, Eduardo Rocha, Kshitij Girigoudar

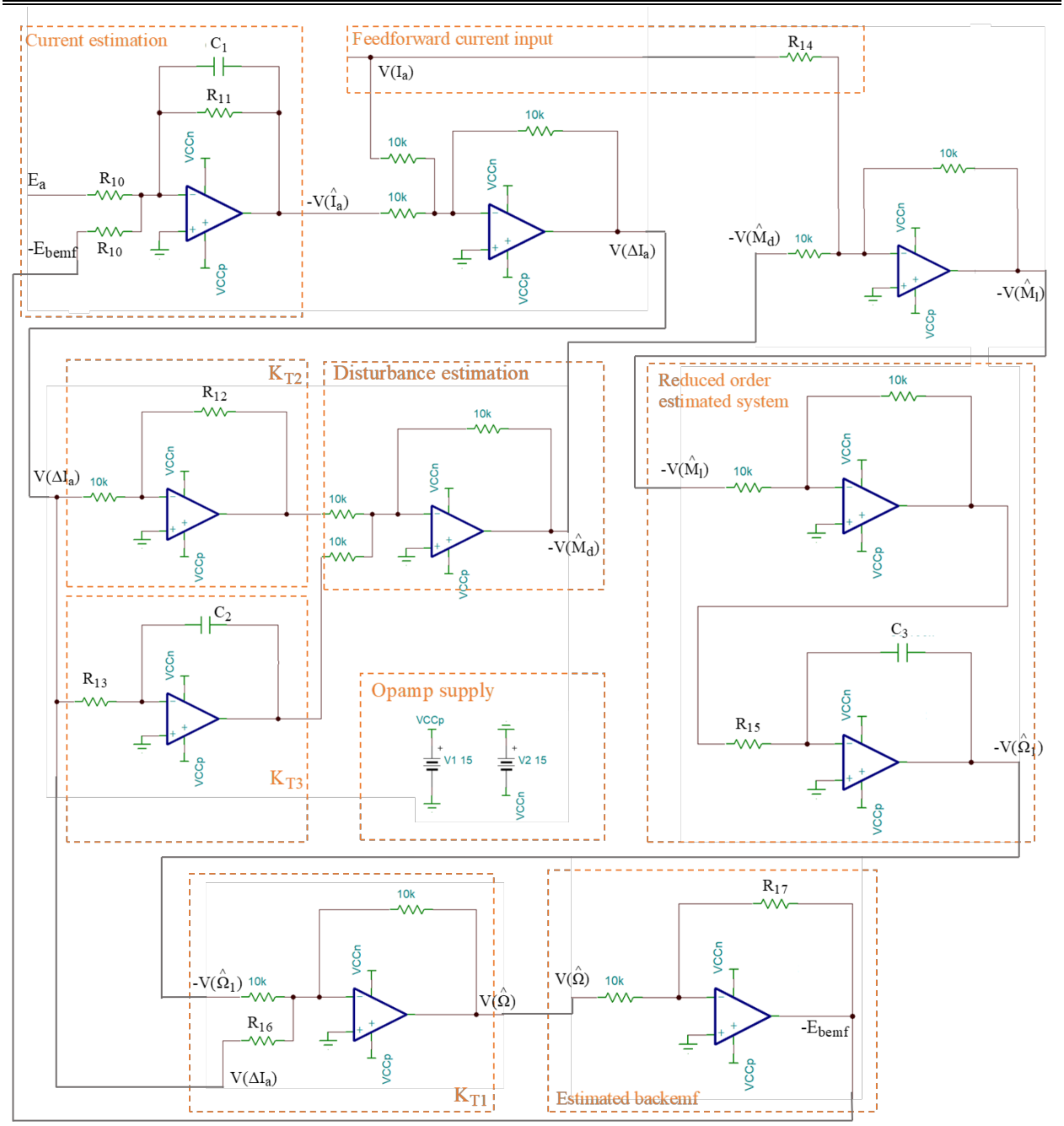

Fig. I.3. Simplified reduced order dc servo motor observer circuit schematic

Previous system implementation with motion state feedback control and the current reference is shown in Fig. I.4. The current reference and voltage feedforward implemented in Lab 5 was disconnected from the circuit. The analog Gopinath observer was integrated into the same circuit as shown in Fig. I.4 to close the loop using estimated velocity in order to achieve self-sensing control.

Analog Gopinath Motion Observer for Velocity Self-Sensing

Austin Gaspar, Eduardo Rocha, Kshitij Girigoudar

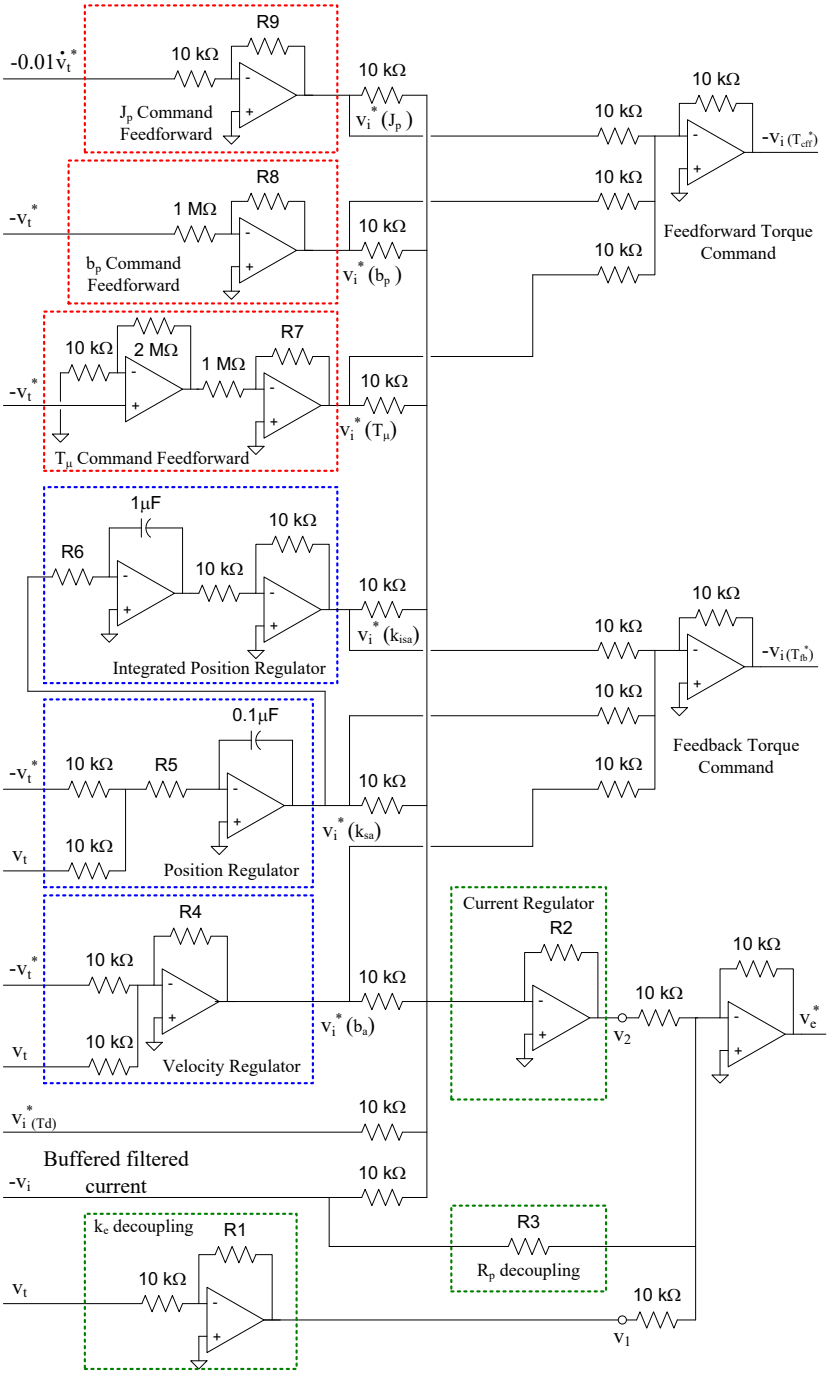

Fig. I.4. Circuit schematic for a state feedback motion controller including a current reference

The following table is a summary of the parameters used in this lab.

Table I.1. Summary of parameters used for tuning

Parameter	Estimation [Units]	Specification [Units]
f_s	Unknown [kHz]	30 [kHz]
V_{dc}	Unknown [V]	50 [V]
k_a	-5.05 [V/V]	-5 [V/V]
R_p	2.96 [Ω]	2.4 [Ω]
L_p	2.88 [mH]	2 [mH]
k_e	0.067 [V-s/rad]	0.054 [V-s/rad]
k_t	0.067 [N-m/A]	0.054 [N-m/A]
J_p	2.08×10^{-5} [kg-m^2]	2×10^{-5} [kg-m^2]
b_p	3.45×10^{-5}[N-m-s/rad]	6×10^{-5} [N-m-s/rad]
k_v	0.016 [V-s/rad]	0.013 [V-s/rad]
k_i	0.41 [V/A]	0.5 [V/A]
T_μ	0.0136 [N-m]	0.01 [N-m]

Table I.2 Summary of gains and resistors

Resistor Values		Equivalent Physical Values		Corresponding eigenvalues, if applicable	
R_1	6.8 [kΩ]	$\hat{k}_e$	0.067 [V-s/rad]	N/A	
R_2	60 [kΩ]	R_a	6.0 [Ω]	EV_{R_a}	500 [Hz]
R_3	6.8 [kΩ]	$\hat{R}_p$	2.96 [Ω]	N/A	
R_4	46 [kΩ]	b_a	0.0122 [N-m-s/rad]	EV_{b_a}	50 [Hz]
R_5	330 [kΩ]	k_{sa}	0.369 [N-m/rad]	$EV_{k_{sa}}$	5 [Hz]
R_6	200 [kΩ]	k_{isa}	1.845 [N-m/rad-s]	$EV_{k_{isa}}$	1 [Hz]
R_{10}	13.91 [kΩ]	$\hat{R}_p$	2.96 [Ω]	N/A	
R_{11}	9.73 [kΩ]	$\hat{L}_p$	2.88 [mH]	N/A	
R_{16}	8.35 [kΩ]	K_{T1}	-6.38×10^{-4} [N-m/A.s/rad]	$EV_{K_{T1}}$	50 [Hz]
R_{12}	176.49 [Ω]	K_{T2}	0.018 [N-m/A]	$EV_{K_{T2}}$	10 [Hz]
R_{13}	1.0 [MΩ]	K_{T3}	0.222 [N-m/A.rad/s]	$EV_{K_{T3}}$	2 [Hz]
R_{14}	149.25 [kΩ]	$\hat{K}_t$	0.067 [N-m/A]	N/A	
R_{15}	5.33 [kΩ]	$\hat{J}_p$	2.08×10^{-5} [kg-m^2]	N/A	
R_{17}	8.29 [kΩ]	$\hat{K}_e$	0.067 [N-m/A]	N/A	

Part 1: Open-loop Current Estimation within the Gopinath Observer (AENG)

Any time a control scheme with several parts is being assembled, the best assembly method is to choose one component, assemble it, and test it thoroughly before continuing to the next. The starting point for this Gopinath observer is the armature circuit estimator. After the armature circuit estimator is working under locked-rotor conditions at all command voltage frequencies, the velocity feedback signal within the observer can be tuned.

A. Locked Rotor Armature Circuit Current Estimation (AENG)

The locked rotor armature circuit is emulated using a single op amp, as was described in the introduction. This op amp is also responsible for summing the velocity feedback path and the command voltage, but the velocity feedback is disconnected and the rotor is locked for all tests in this section.

By the way the circuit was designed, the relationship between the circuit resistances and capacitance and the estimated armature resistance and inductance is provided by (1.A.1)-(1.A.4).

$$\frac{V_i(I_a)(s)}{V_e^*(s)} = \frac{k_a k_i}{L_p s + R_p} \tag{1.A.1}$$

$$\frac{\hat{V}_i(I_a)(s)}{V_e^*(s)} = \frac{R_{11}}{R_{10}} \frac{1}{R_{11}C_1 s + 1} \tag{1.A.2}$$

$$\hat{L}_p = \hat{k}_a \hat{k}_i R_{10} C_1 \tag{1.A.3}$$

$$\hat{R}_p = \frac{\hat{k}_a \hat{k}_i R_{10}}{R_{11}} \tag{1.A.4}$$

Two FRF's can be used to tune the current estimator. First, the actual and estimated relationship between voltage and current can be compared. If the estimated FRF overlaps the actual FRF, then the tuning is correct. Several FRF tunings are captured and overlaid with each other and the actual locked rotor armature circuit FRF in Fig. 1.A.1. The rotor is locked since the current estimator op amp does not include the velocity feedback.

Analog Gopinath Motion Observer for Velocity Self-Sensing

Austin Gaspar, Eduardo Rocha, Kshitij Girigoudar

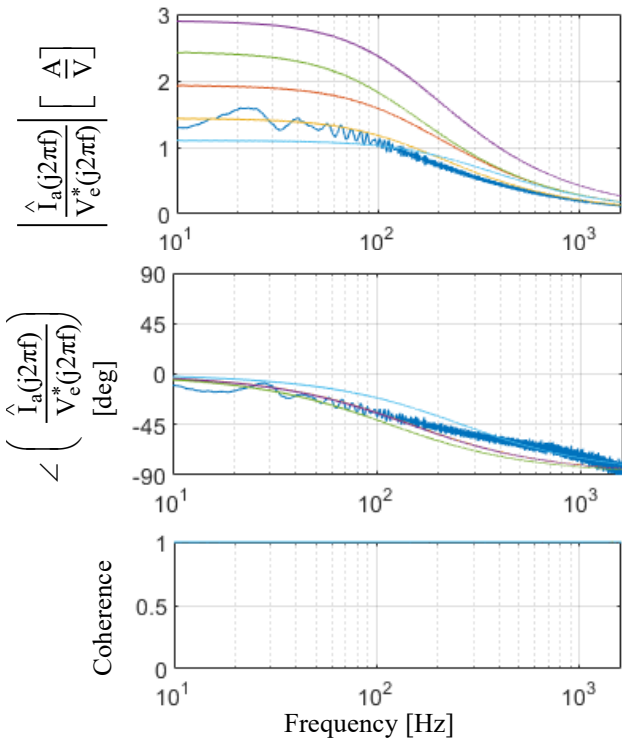

Legend:

Actual Armature Circuit

R_{10}=15kΩ, R_{11}=10kΩ, C_1=0.1μF, $\hat{R}_p$=3.1Ω, $\hat{L}_p$=3.1mH

R_{10}=20kΩ, R_{11}=10kΩ, C_1=0.1μF, $\hat{R}_p$=4.1Ω, $\hat{L}_p$=4.1mH

R_{10}=10kΩ, R_{11}=10kΩ, C_1=0.1μF, $\hat{R}_p$=2Ω, $\hat{L}_p$=2mH

R_{10}=15kΩ, R_{11}=15kΩ, C_1=0.1μF, $\hat{R}_p$=2Ω, $\hat{L}_p$=3.1mH

R_{10}=15kΩ, R_{11}=6.8kΩ, C_1=0.1μF, $\hat{R}_p$=4.5Ω, $\hat{L}_p$=3.1mH

Test Conditions:

V_e^* = chirp, $1V_{rms}$ amplitude, $0V_{DC}$ offset, 0.1-1600Hz

4sec sweep

Locked Rotor

FFT Settings:

1.6kHz span, f_b = 0.25Hz, uniform window, 3 freq averages (10 freq averages for actual armature circuit)

Fig. 1.A.1: Overlaid locked rotor armature circuit FRF and observer estimated armature circuit FRFs

The other FRF that can be used to analyze the current estimation is an estimation accuracy FRF. Using this plot, the estimation of current is ideal when the estimation accuracy FRF has a magnitude of one and zero phase distortion across all frequencies. The estimation accuracy FRF for the same conditions as Fig. 1.A.1 is provided in Fig. 1.A.2.

Both plots concur that the best estimate for the armature circuit estimator occurs when $\hat{R}_p$=4.1Ω and $\hat{L}_p$=4.1mH. The magnitude of the estimation accuracy plot increases at low frequencies when the armature resistance is underestimated, and it increases at high frequencies when armature inductance is underestimated. While both plots offer a way to verify the tuning of the estimated armature circuit, the estimation accuracy plot is directly and independently manipulated with varying estimations of inductance and resistance.

Analog Gopinath Motion Observer for Velocity Self-Sensing

Austin Gaspar, Eduardo Rocha, Kshitij Girigoudar

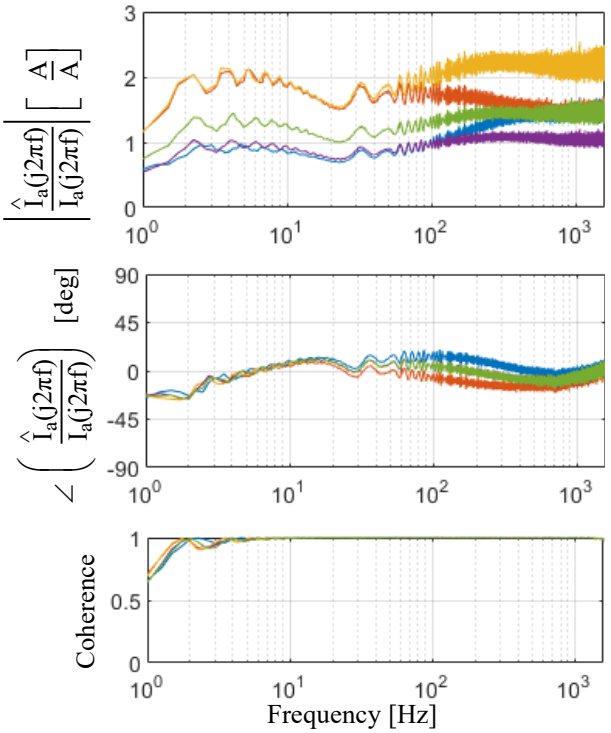

Legend:

R_{10}=15kΩ, R_{11}=10kΩ, C_1=0.1μF, $\hat{R}_p$=3.1Ω, $\hat{L}_p$=3.1mH

R_{10}=20kΩ, R_{11}=10kΩ, C_1=0.1μF, $\hat{R}_p$=4.1Ω, $\hat{L}_p$=4.1mH

R_{10}=10kΩ, R_{11}=10kΩ, C_1=0.1μF, $\hat{R}_p$=2Ω, $\hat{L}_p$=2mH

R_{10}=15kΩ, R_{11}=15kΩ, C_1=0.1μF, $\hat{R}_p$=2Ω, $\hat{L}_p$=3.1mH

R_{10}=15kΩ, R_{11}=6.8kΩ, C_1=0.1μF, $\hat{R}_p$=4.5Ω, $\hat{L}_p$=3.1mH

Test Conditions:

V_e^* = chirp, $1V_{rms}$ amplitude, $0V_{DC}$ offset, 0.1-1600Hz 4sec sweep
Locked Rotor

FFT Settings:

1.6kHz span, f_b = 0.25Hz, uniform window, 3 freq averages

Fig. 1.A.2. Locked rotor current estimation accuracy FRFs

B. Adding velocity feedback to the armature estimator (AENG)

Since the current estimate is now accurate at all frequencies when the rotor is locked, the next step is to make the current estimate accurate at all velocity operating conditions. To do this, the $\hat{k}_e$ estimate in the Gopinath velocity feedback needs to be tuned. The gain calculation is provided by (1.B.1)-(1.B.3).

$$\frac{V_{bemf}}{V_t} = \frac{k_e}{k_v k_a} \tag{1.B.1}$$

$$\frac{\hat{V}_{bemf}}{V_t} = \frac{R_{17}}{10k\Omega} \tag{1.B.2}$$

$$\hat{k}_e = \frac{R_{17}\hat{k}_v\hat{k}_a}{10k\Omega} \tag{1.B.3}$$

Since no estimation of velocity has been created yet, the tachometer voltage is used instead to tune R_{17}. A very low frequency, high amplitude sine wave voltage is applied to the voltage command, allowing a large range of operating speeds to be explored at approximately steady state. The estimated current and actual current is overlaid for various tunings of R_{17}, as shown in Fig. 1.B.1.

Analog Gopinath Motion Observer for Velocity Self-Sensing

Austin Gaspar, Eduardo Rocha, Kshitij Girigoudar

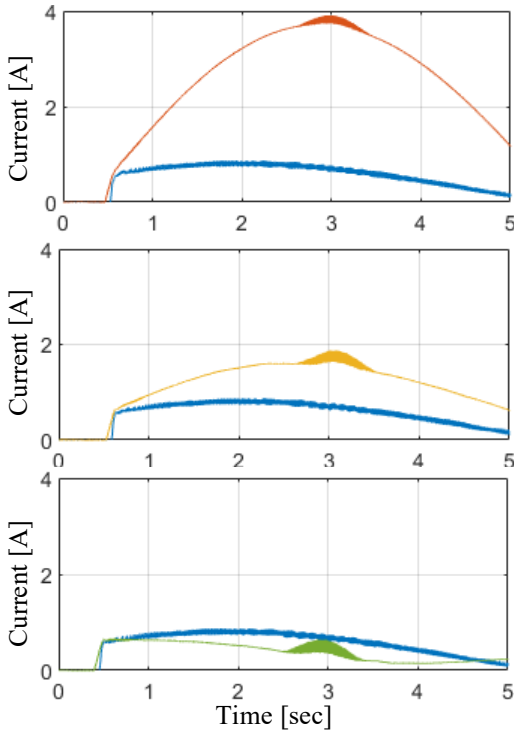

Fig. 1.B.1. Steady state current estimation for a wide range of operating speeds and various tunings of R_{17}

Clearly, a tuning of $R_{17} = 10k\Omega$, or $\hat{k}_e = 0.080$ V-s/rad, shows the best tuning since the difference between the estimated current and measured current is smallest. The tuning of this gain is indifferent to frequency since it is a simple proportional gain, so if the current estimate is accurate at any velocity at steady state, and it is accurate at any frequency when the rotor is locked, then the current estimate will be accurate at any operating speed and frequency.

Part 2: Physical Inertia Estimate Tuning (AENG)

To tune the physical inertia estimate, the rest of the circuit (minus the K_{T1} path) must be built. The physical inertia estimate is tested by checking the estimation accuracy of the velocity using only the torque command feedforward, but attempting this alone can cause instability since an integrator exists between the torque and the velocity. To ensure stability, the velocity estimate must be closed loop and the entire observer must be built. If the observer bandwidth is low, then the command feedforward will dominate at any frequency higher than the bandwidth. This will allow the physical inertia estimate to be directly tuned. The physical inertia estimate is related to the op amp circuit by (2.1)-(2.3).

$$\frac{V_t(\Omega)(s)}{V_i(M_e)(s)} = \frac{k_v}{k_i J_p s} \tag{2.1}$$

$$\frac{\hat{V}_t(\Omega)(s)}{\hat{V}_i(M_e)(s)} = \frac{1}{R_{15}C_3 s} \tag{2.2}$$

$$\hat{J}_p = \frac{R_{15}C_3\hat{k}_v}{\hat{k}_i} \tag{2.3}$$

In this part of the observer construction, observer eigenvalues are unimportant as long as they are not too high and do not cause overwhelming oscillatory behavior. The entire observer is built with a low bandwidth. A velocity estimation accuracy FRF is shown in Fig. 2.1.

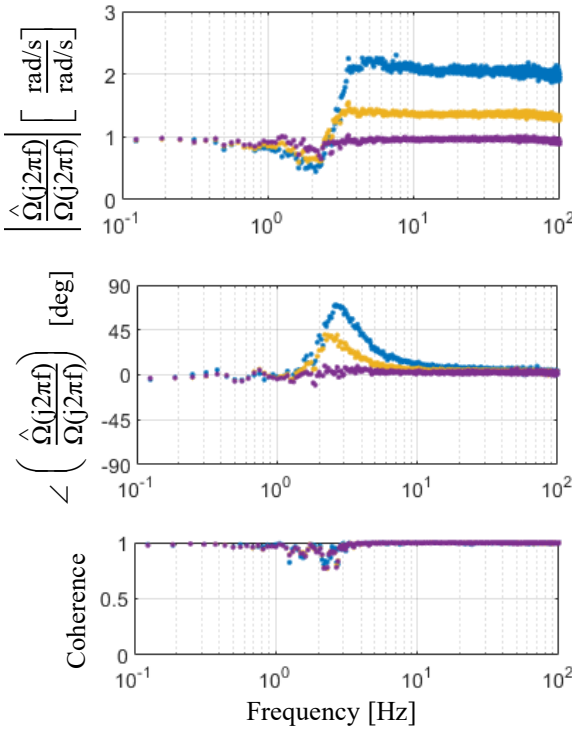

Legend:
R_{15} = 4.7kΩ, $\hat{J}_p$ = 18.3 mg-m^2
R_{15} = 6.8kΩ, $\hat{J}_p$ = 26.5 mg-m^2
R_{15} = 10kΩ, $\hat{J}_p$ = 39.0 mg-m^2

R_{10} = 20kΩ, R_{11} = 10kΩ, R_{12} = 200Ω, R_{13} = 1MΩ, R_{14} = 150kΩ, R_{17} = 10kΩ, C_1 = 0.1μF, C_2 = 2μF, C_3 = 0.1μF
$\hat{R}_p$=4.1Ω, $\hat{L}_p$=4.1mH, $\hat{k}_e$ = 0.080 V-s/rad, $\hat{k}_t$ = 0.067 N-m/A,
K_{T2} = 0.5 N-m/A,
K_{T3} = 0.02 N-m-s/rad-A
Observer EV's: 1.1, 4.0 Hz

Test Conditions:
E_a = random noise, 1V_{rms} amplitude, 2V_{DC} offset, 0-100Hz

FFT Settings:
100Hz span, f_b = 62.5mHz, Hanning window, 10 freq averages

Fig. 2.1. Velocity Estimation Accuracy while tuning R_{15} ($\hat{J}_p$)

As the physical inertia estimate is increased, the high frequency estimation accuracy magnitude response is reduced. This Gopinath velocity estimation accuracy is incredibly similar to the estimation accuracy of a Luenberger observer. The low frequency magnitude response is unity and the phase has zero lead/lag at both high and low frequencies. Although this Gopinath observer has unity low frequency magnitude estimation accuracy, a poorly tuned Gopinath observer will not have a unity gain. The low frequency response is independent of the physical inertia estimate, but dependent on the estimation of $\hat{k}_e$. Since this parameter was well estimated in part 1.B, the low frequency estimation accuracy appears ideal. If the parameter was over estimated, then the estimated back-EMF voltage would be higher than actual. This would cause the observer to estimate a lower velocity than what is actually present at steady state. This is important to note because Gopinath observers cannot estimate an unmeasured state with zero steady state error without ideal parameter estimation.

At the Gopinath observer's break frequency of 4 Hz, the estimation accuracy plot transitions to its higher frequency estimate which is solely dependent on the torque command feedforward. This behavior, along with the bump in phase lead/lag at the break frequency, is analogous to Luenberger observers. The physical inertia estimate is tuned by watching the high frequency magnitude estimation accuracy and manipulating the estimate until the high frequency estimation accuracy becomes unity. Because of the way the observer is constructed, the phase lead/lag will naturally be zero across all frequencies.

One caveat to this method is that it assumes the torque command feedforward is ideal. In reality, the torque command feedforward is sensitive to the estimate of $\hat{k}_t$. If this parameter is not well known, then the newfound tuning for the physical inertia estimate only demonstrates that the ratio between $\hat{k}_t$ and $\hat{J}_p$ is tuned correctly. The consequence of not knowing these parameter estimates individually is an inaccurate torque disturbance estimate, $\hat{M}_d$. If an accurate torque disturbance estimate is needed, then $\hat{k}_t$ can be tuned while keeping the $\hat{k}_t/\hat{J}_p$ ratio constant. When $\hat{M}_d$ is approximately zero for any steady-state velocity without an applied disturbance, then $\hat{k}_t$ is tuned correctly. This was not done due to time constraints during the Gopinath observer implementation.

Part 3: Observer Eigenvalues Tuning (EMCR)

This part focuses in the tuning of the observer eigenvalues. As seen in the introduction, the observer eigenvalues can be calculated by the polynomial denominator of the observer estimation accuracy transfer function, seen in (3.1).

$$\hat{J}_p \hat{L}_p s^3 + (\hat{J}_p \hat{R}_p + \hat{K}_e K_{T1}) s^2 + \hat{K}_e K_{T2} s + \hat{K}_e K_{T3} \tag{3.1}$$

Based in this model, the observer gains for desired eigenvalues $[f_1, f_2, f_3]$ can be calculated by equations (3.2), (3.3) and (3.4).

$$K_{T1} = \frac{\hat{J}_p \hat{L}_p 2\pi f_1 - \hat{J}_p \hat{R}_p}{\hat{K}_e} \tag{3.2}$$

$$K_{T2} = \frac{2\pi f_2 (\hat{J}_p \hat{R}_p + \hat{K}_e K_{T1})}{\hat{K}_e} \tag{3.3}$$

$$K_{T3} = 2\pi f_3 K_{T2} \tag{3.4}$$

The gain values were calculated for eigenvalues of [2Hz, 10Hz, 50Hz]. In order to see the observer real eigenvalues, the dynamic stiffness FRF of the observer, $I_a(j2\pi f)/\hat{\Omega}(j2\pi f)$, was plotted. Then, the gains K_{T1}, K_{T2} and K_{T3} were tuned in order to achieve the desired behavior. The dynamic stiffness FRFs obtained for different tunings can be seen in Fig 3.1.

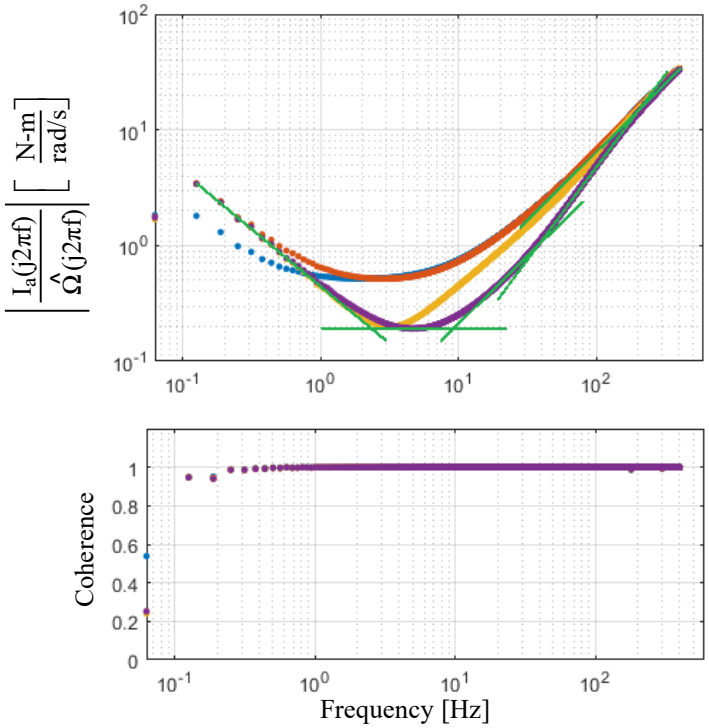

Legend:
R_{12} = 1kΩ, R_{13} = 1MΩ, R_{16} = 10kΩ, C_2 = 4μF
R_{12} = 1kΩ, R_{13} = 1MΩ, R_{16} = 10kΩ, C_2 = 2μF
R_{12} = 0.39kΩ, R_{13} = 1MΩ, R_{16} = 6.8kΩ, C_2 = 2μF
R_{12} = 0.39kΩ, R_{13} = 1MΩ, R_{16} = 4.7kΩ, C_2 = 2μF
Asymptotes to final tuning

R_{10} = 20kΩ, R_{11} = 10kΩ, R_{14} = 150kΩ, R_{15} = 10kΩ, R_{17} = 10kΩ, C_1 = 0.1μF, C_3 = 0.1μF

Test Conditions:
$V_i(I_a)$ = random noise, $1V_{rms}$ amplitude, $0V_{DC}$ offset, 0.1-400Hz span

FFT Settings:
400Hz span, f_b = 0.0625Hz, Hanning window, 10 freq averages

Fig. 3.1. Observer Dynamic Stiffness FRFs for different gain tunings.

The closest to the desired eigenvalues of [2Hz, 10Hz, 50Hz] obtained were the eigenvalues [2.3Hz, 9Hz, 36Hz], as seen in Fig 3.1. The calculated resistor values for the eigenvalues desired and the values obtained in the tuned system can be seen in Table 3.1.

Table 3.1. Observer gains calculated and tuned for desired eigenvalues

	R_{12} [Ω]	R_{13} [MΩ]	R_{16} [kΩ]	K_{T1} [N-m-rad/A-s]	K_{T2} [N-m/A]	K_{T3} [N-m-s/rad-A]
Calculated values for [2Hz, 10Hz, 50Hz]	176.5	2.25	8.35	-6.38e-4	0.0176	0.2218
Obtained values for [2.3Hz, 9Hz, 36Hz]	390	1	4.7	-0.0011	0.0390	0.5

It can also be seen in Fig 3.1 that independently of the tuning, all FRFs obtained overlay in the same asymptote for high frequencies. It occurs because it is past the observe bandwidth.

Part 4: Sensor- versus Observer-Based State Feedback on the State Feedback Motion Controller (EMCR)

This part focuses in the comparison between the observer estimated velocity and the tachometer velocity as feedback for the motion controller. The comparison is made by the over plot of command tracking and dynamic stiffness FRFs.

A. Command Tracking Comparison (EMCR)

The command tracking FRF was obtained for both sensor-based state feedback and observer-based state feedback. During data collection, it was hard to obtain an FRF with good coherence for low and high frequencies using observer estimated velocity. Therefore, it was obtained separated FRFs for low and high frequencies. The results obtained can be seen in Fig 4.1.

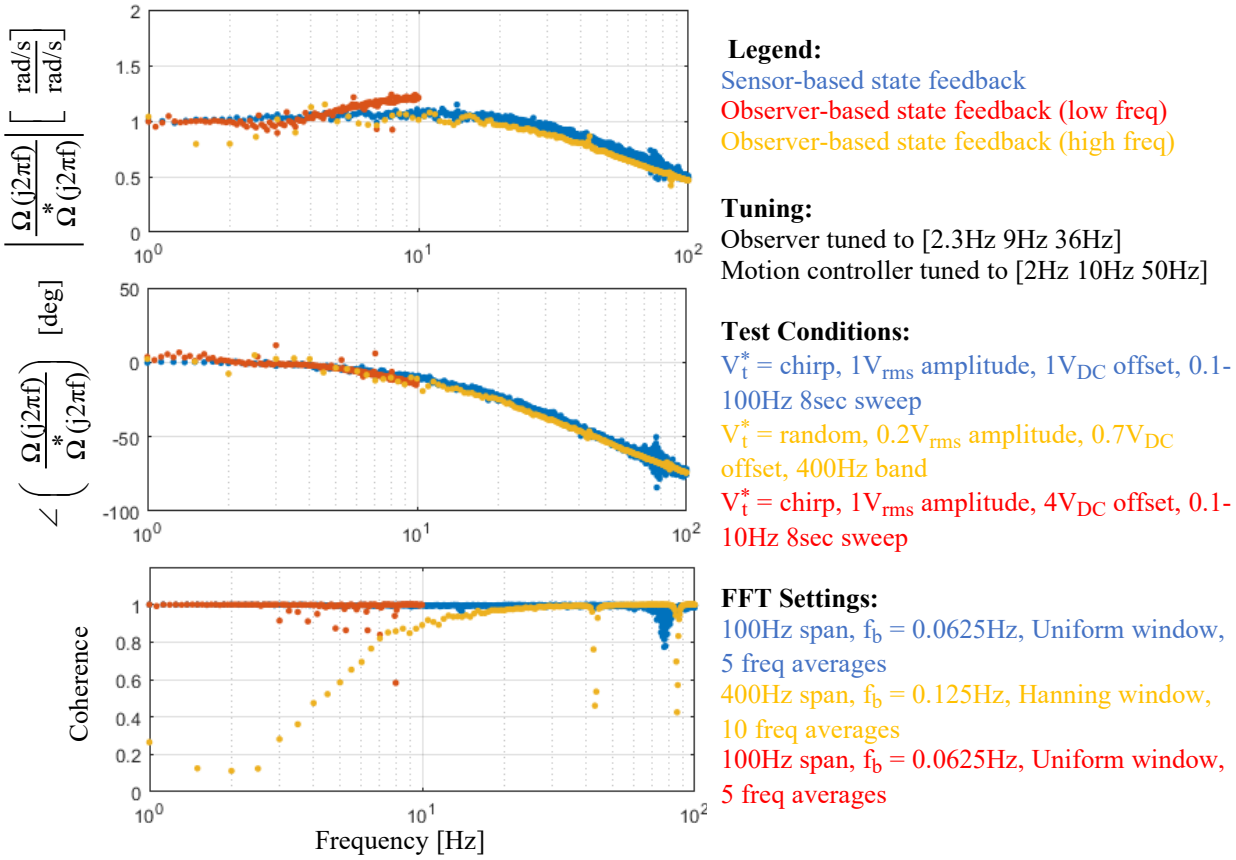

Fig. 4.1. Closed-loop command tracking FRFs for different state feedback

It can be seen in Fig 4.1 that the command tracking is very similar for the two cases. It shows that the correct behavior of the Gopinath observer.

B. Dynamic Stiffness Comparison (EMCR)

The dynamic stiffness FRF was obtained for both sensor-based state feedback and observer-based state feedback. It was hard to obtain an FRF with good coherence for all frequencies using observer estimated velocity. So, it was obtained separated FRFs for different frequency bands. The results obtained can be seen in Fig 4.2.

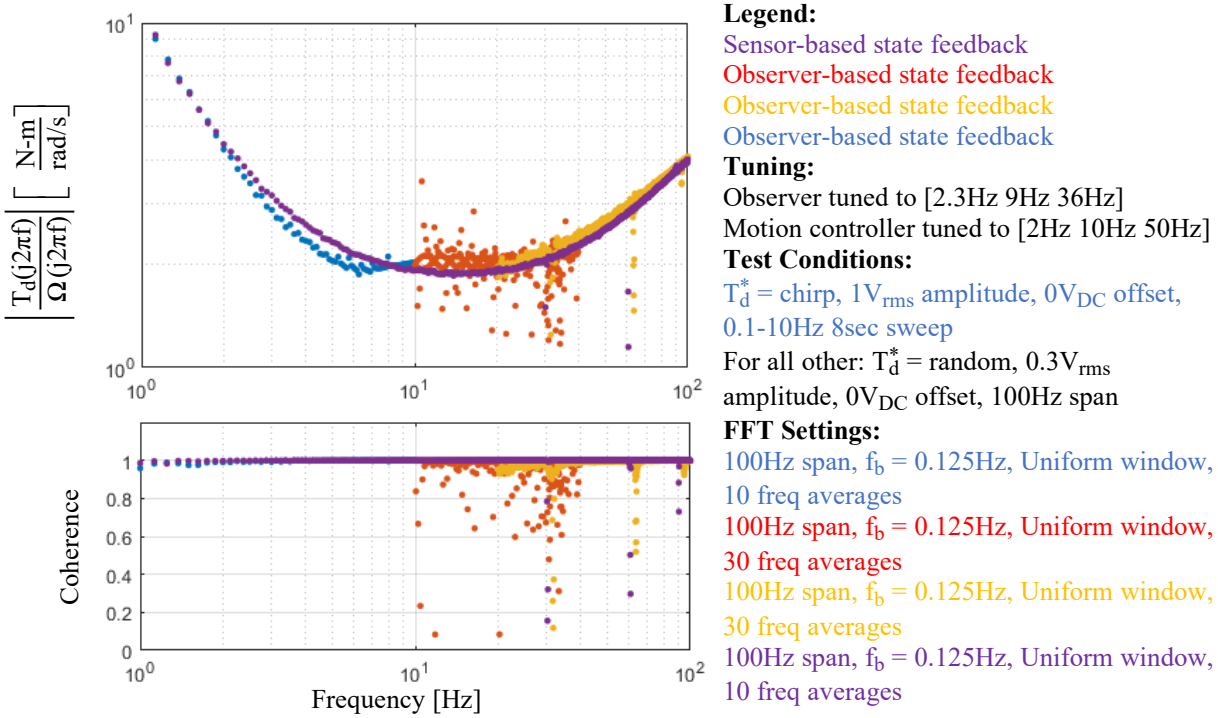

Fig. 4.2. Closed-loop dynamic Stiffness FRFs for different state feedback

It can be seen in Fig 4.2 that, as command tracking, the dynamic stiffness FRFs are very similar for both cases. It shows that the observer was capable to replace the sensor without compromising command tracking and dynamic stiffness. It shows the importance of this type of observer that, differently from the Luenberger observer, allows self-sensing control, which is better for some applications. It can save money and space.

Part 5. Summary

A. Summary of Parameters (KG)

Table 5.1 is a summary of the gains and resistor values used to achieve the desired tuning for this lab.

Table 5.1. Resistance and gains used in the control circuit

Parameter	Calculated Value [Units]	Experimental Values (after tuning) [Units]
R_1	8.4 [kΩ]	6.8 [kΩ]
R_2†	23.7 [kΩ]	60 [kΩ]
R_3	7.0 [kΩ]	6.8 [kΩ]
R_4	43.3 [kΩ]	46 [kΩ]
R_5	318.3 [kΩ]	330 [kΩ]
R_6	159.1 [kΩ]	200 [kΩ]
R_7	6.402 [kΩ]	4.7 [kΩ]
R_8	13.195 [kΩ]	20 [kΩ]
R_9	7.955 [kΩ]	12 [kΩ]
R_{10}	13.91 [kΩ]	20 [kΩ]
R_{11}	9.73 [kΩ]	10 [kΩ]
R_{12}	176.49 [Ω]	390 [Ω]
R_{13}	1.0 [MΩ]	1 [MΩ]
R_{14}	149.25 [kΩ]	150 [kΩ]
R_{15}	5.33 [kΩ]	10 [kΩ]
R_{16}	8.35 [kΩ]	4.7 [kΩ]
R_{17}	8.29 [kΩ]	10 [kΩ]
K_{T1}	-6.38×10^{-4} [N-m/A.s/rad]	-0.0011 [N-m/A.s/rad]
K_{T2}	0.018 [N-m/A]	0.039 [N-m/A]
K_{T3}	0.222 [N-m/A.rad/s]	0.5 [N-m/A.rad/s]

† after R_p Decoupling NA- Experiment not done

B. Conclusion (AENG/EMCR/KG)

The objective of this project was to investigate the performance of a Gopinath observer for velocity estimation. Compared to the noise of the tachometer feedback, observer will provide a much cleaner velocity estimate and also filter out the noise content in the measured current. The bandwidth of the observer must be chosen depending on whether a higher dynamic stiffness (high bandwidth) is required or a better noise filtering capability (low bandwidth) is necessary. The added parameter sensitivity in the Gopinath observer makes the system identification extremely important. Since the observer also estimates disturbance torque, it can be used to improve the dynamic stiffness further by implementing DID. Due to time constraints, this was not implemented in the lab. (KG)

A practical Gopinath observer should be built one step at a time. After each "block" is built, the block should be tuned so it behaves as ideally as possible. Tuning the blocks in the order presented in this paper will allow each estimated parameter to be isolated from the effects of surrounding parameter estimates (decoupled). The current estimator can be tuned using an estimation accuracy plot, the back-emf constant can be estimated using the current estimate in the time domain, and the inertia can be estimated by looking at the velocity estimate at high frequencies. (AENG)

The Gopinath observer dynamic stiffness was used in order to tune the observer to the desired bandwidth. The resistor values calculated and obtained after the tuning are similar, off by a factor of 2. After the tuning, the observer was used as state feedback for the closed loop system. The results were compared with the results obtained with tachometer feedback. It was obtained that the use of the observer did not compromise the dynamic stiffness and the command tracking of the system, showing that the observer was correctly implemented. It was verified the correct working of the closed-loop system without a position or velocity sensor. (EMCR)